# HIGH-SPEED DIGITAL SHADOWGRAPHY FOR HIGH-FREQUENCY SHOCK TRACKING IN SUPERSONIC FLOWS

B.H. Timmerman, P.J. Bryanston-Cross, A.J. Skeen, P.G. Tucker*, R.J. Jefferson-Loveday, P. Dunkley

Optical Engineering Laboratory, University of Warwick, Coventry CV4 7AL UK
* Currently at Civil and Computational Engineering Centre, University of Wales, SA2 8PPSwansea

J. Paduano, G.R.Guenette.Jr

Gas Turbine Laboratory, Massachusetts Institute of Technology, Cambridge, MA, USA 02139

## ABSTRACT

A digital focused shadowgraph visualization system has been developed to provide an optical diagnostic for unsteady high-speed flows. The technique is particularly designed for tracking shock positions in a supersonic inlet. It provides a direct electronic output that represents shock position, enabling high-speed active shock control.

The system features three modes of operation:

- High-resolution digital still frames and sequences
- High-resolution digital frames and sequences showing the spatial-temporal variation in the flow field
- Adjustable windowed digital frames enabling high-speed active shock control

Measurements and predictive calculations are presented of the unsteady shock around an aspirated cone-shaped nozzle. The system is based on a low-cost high intensity white LED light source and a CMOS digital camera. The camera, which can be programmed for variable resolution and framing rate, transmits the shock position data directly to the memory of a computer and provides a direct electronic output of the shock position at up to 980Hz.

The measured results are compared to results from numerical simulations based on the high accuracy NTS Navier-Stokes solver and Roe's flux difference splitting method. Good correspondence between measured and numerical shock position and angle is found.

## INTRODUCTION

A flow visualization system was designed to provide a fast, low-cost and easy-to-use diagnostic for aerodynamic design concepts to be tested in the supersonic wind tunnel at the Gas Turbine Laboratory at MIT. Besides providing a general flow visualization capability, it is designed specifically for tracking high-speed unsteady events in a supersonic flow.

One of the investigations taking place at MIT is the design of an efficient supersonic inlet. One approach to increasing the efficiency of a gas turbine engine is to actively control the position of the intra-passage shock wave. A major design driver for supersonic diffusers is the requirement to prevent unwanted shock formation and shock blow-out (supersonic unstart). As part of the Quiet Supersonic Platform (QSP) program (DARPA, 2003) to create a new efficient supersonic vehicle in the business jet size range, efficient supersonic inlets are being designed that rely on feedback control, rather than traditional design methods, to prevent unstart. To aid in the design and to study the dynamics and control of shock formation and movement, high-speed tracking of shocks is needed. This typically requires a positional shock measurement resolution better than 0.2 mm and temporal resolution in the ms range. Furthermore, to create an active flow control device the positional data needs to be transmitted at a rate in the region of 1kHz.

The measurement technique developed here for dynamical shockwave-tracking is based on a low-cost, robust digital shadowgraphy assembly. The developed system provides both a global visualization needed for initial determination of the approximate shock position, as well as a high-speed tracking of shock-wave position at rates up to 1 kHz based on a zoomed view of the shock region. Because of the unsteadiness in the flow, individual images need to be recorded at short exposure times (microseconds), in order to 'freeze' the instantaneous events and avoid motion-blurring.

Shadowgraphy, as a well-established technique for compressible flow field visualization (e.g. Merzkirch 1987), especially in visualizing shock waves, was chosen as a basis in order to build a

robust system with a minimal number of optical components. Furthermore, the use of a focused shadowgraphy system allows accurate determination of the actual position of shock waves in the flow.

The direct digital recording of the shadowgraph images allows a direct processing, in this case used for on-line real-time determination of shock wave position. This real-time information can then be used for direct-control feedback, e.g. to change flow settings in order to control the shock formation in a supersonic inlet.

High-speed flow visualization systems have been reported before. However, for a long time, high-frame rates could generally only be achieved by the use of specialized systems such as drum-cameras (Donohoe and Bannink, 1997; Timmerman, 1997). Direct digital imaging, however, has often been limited to recording only a few images at the high rate (Ben-Yakar and Hanson, 2002). For longer sequences at high resolution, the digital recording rate is generally limited by the 25/30 Hz framing rate of standard cameras, or requires the use of expensive dedicated cameras (Gord *et al.*, 1998). Besides being expensive, such cameras have a short technology lifetime. Alternatively, high-speed tracking has been achieved using photodiode systems, however these 1-D systems will only give information on a single point rather than an area in the flow.

In the set-up presented here, a CMOS-type cameras is used. CMOS cameras offer the advantage of being relatively low-cost (compared to CCD-type) while still allowing high-speed tracking to be achieved. The CMOS camera used here does not have a global electronic shutter, which allows a new type of imaging, spatial-temporal streak imaging, which provides information on both temporal as well as spatial variation.

The described system shows a direct method not previously explored to provide an active shock control within a transonic test facility. The system is tested on an aspirated cone-shaped nozzle placed in a supersonic wind tunnel flow. By varying the jet flow generated by the nozzle, the bow-shock around the cone is modulated, generating a high-frequency oscillation of the bow shock.

The measured results are compared to results from numerical simulations. The axisymmetric simulations are made with a high accuracy compressible flow solver (Tucker, 2004). Solutions are advanced in time using a 2nd order implicit backwards differentiation. For the non-linear spatial derivatives Roe's scheme is used. For this, underlying interpolations can be up to $5^{th}$ order accuracy. The code is run in parallel processor mode with a dual block grid. To resolve the more intricate flow features around the pulsating jet region an especially fine inner block grid is used. Because of the low geometrical complexity the grid is algebraically generated.

## NOMENCLATURE

LED: Light Emitting Diode

CMOS: Complementary Metal Oxide Semiconductor

## HIGH-SPEED IMAGING USING CMOS CAMERA

The detection sensor used here is a Vitana PixeLINK PL-A653 mega-pixel CMOS camera. The ½" monochrome sensor has a maximum resolution of 1280×1024 pixels, but different window-sizes can be chosen, down to a minimum sub-window of 32x8 pixels at 8- or 10-bit depth. Moreover, the position of these windows can be chosen arbitrarily. The maximum framing-rate depends on the size of the chosen window with a full-resolution frame-rate of 12fps at 8-bit image depth. Furthermore it provides a single cable FireWire connection, reading the image data directly into the memory of the host computer (400 Mbits/second), eliminating the need for a data-acquisition card.

An important feature of this camera is that the sensor lacks a global electronic shutter. The pixels in the sensor do not capture data at the same time, but rather are exposed pixel-by-pixel, row-by-row. As a consequence, the images that are captured are not instantaneous, but show a time delay between the rows. The start of each pixel's integration is staggered by the inverse of the pixel clock (up to 24MHz). When operating the camera at full-frame resolution this results in adjacent rows depicting events approximately 80μs apart.

By changing the camera settings it is possible to operate the shadowgraphy system in three separate modes: still view mode, spatial-temporal streak view mode and tracking view mode. Each of these modes produces a different type of result.

*Spatial-Temporal Streak View*

Running the camera in video mode results in images akin to those from a streak camera, i.e. the time at which the event is captured varies along the rows of the picture. Unlike a streak camera however, the captured image is not a one-dimensional strip but the whole two-dimensional area under investigation, i.e. each pixel in the image represents a different location as well as a different moment in time. The authors have therefore dubbed the result "spatial-temporal streak" images, and have found them to be a useful way to visualize, in real-time, the movement of shock waves that are oscillating at a speed that is otherwise difficult to capture.

Despite the fact that images are not taken instantaneously in this mode, the effect of motion blur in the images that are captured is limited to

extremely high-speed events, and in general the data does not suffer from motion blur. In the case studied in this paper, with the camera positioned such that the shock waves run primarily along the vertical axis of the image, the shock typically oscillates no more than ±10 pixels side to side. At full-frame resolution, the sensor takes 1.2µs to sample 20 adjacent pixels, meaning that a shock would have to oscillate at over 20kHz before the readout rate causes rows to become motion-blurred by more than 1 pixel. While each row can therefore be considered an instantaneous view, adjacent rows depict the shock position separated by approximately 80µs with the bottom of the picture representing the most recent position. The result is a 'wobbly' image, updated at 12fps that clearly shows the amplitude and frequency of shock movement.

*Still View Mode*

Without a global electronic shutter the camera is unable to capture an image across the entire sensor instantaneously, resulting in the spatial-temporal images described above. Nevertheless, it is still possible to obtain instantaneous snapshots. For this, the camera is set to integrate for a time longer than the readout period of the whole sensor. For this a controllable flashing light source is needed, illuminating the imaged scene for one instant. At the point when all rows are integrating, the light source is flashed for the desired exposure time. Thus, all pixels are exposed during the same 'instant' (the duration of the flash) and a freeze-frame still image is obtained. The PL-A653 camera provides TTL-level connections to facilitate the control of external flash and shutter mechanisms, but only down to pulses of ~100µs. Therefore, in the experiments described here, an external triggered pulse generator is used allowing the light source (an LED in this case) to be pulsed for periods much shorter than the limit imposed by the camera. In the results shown here, the pulses lasted 10 µs.

Still view mode therefore provides a live stream of instantaneously captured images. While theoretically limited to half of the normal frame rate, i.e. 6 fps for full-frame images, the implemented system ran at 2fps due to the fact the images had to be stored on hard-disk, rather than in RAM.

*Tracking View*

The CMOS sensors can be set to any sub-window size at any position. For a reduced number of pixels, the frame rate increases. At the maximum horizontal and minimum vertical resolution of 1280×8, the frame rate is typically 980fps, with a read-out period of approximately 640µs. To reduce the read-out time for the results shown here, only the last 4 rows of this sub-window were considered, resulting in an acquisition time of 320µs, or approximately 1⁄8 of a 400Hz oscillation period (for a negligible exposure period). A smaller horizontal resolution further reduces the acquisition time, meaning that for the purposes of tracking, the acquisition can be considered to be instantaneous.

## FLOW CONFIGURATION

The characteristics of unsteady shock behavior expected in supersonic inlets are simulated in a supersonic wind tunnel at the Gas Turbine Laboratory of MIT. The test section of this tunnel is

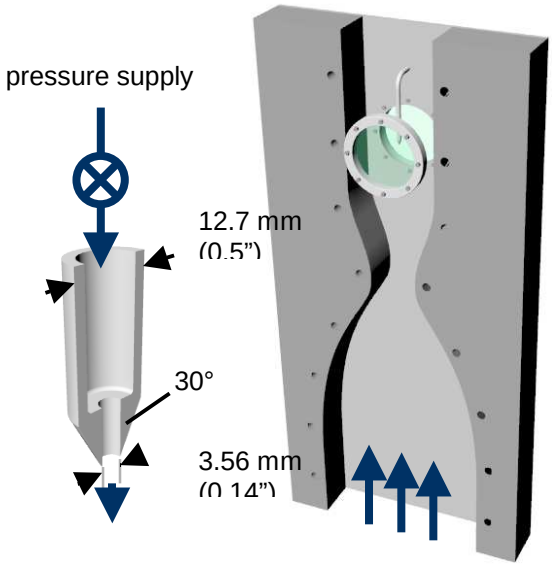


**Figure 1: Aspirated nozzle in supersonic windtunnel**

vertical, with the flow direction upwards and measures 203x203 mm$^2$ (8"x8"). Optical access is provided by two circular windows with a diameter of 133 mm (5¼") in the sidewalls. An aspirated nozzle, shown in Figure 1, was placed in the center of the test section pointing downwards, i.e. in the direction opposite to the tunnel flow. The exit of this nozzle was placed at the level of the center of the optical access windows.

Air can be blown through the nozzle generating an under-expanded free jet flow. With this configuration in the wind tunnel, different types of flow can be studied. Firstly, the wind-tunnel flow around the nozzle, generating a steady shock wave pattern around the spike; secondly, the free jet flow from the nozzle, generating a shock-diamond pattern typical for under-expanded free jets and thirdly a combination of the two. To simulate the unsteady shock movement, the jet flow coming from the nozzle can be modulated by varying the nozzle pressure using a simple rotary valve. This enables modulation of the jet conditions up to several kHz. Thus, the diamond-shock pattern can be modulated and more interestingly, the position of the bow shock in front of the nozzle in the jet-tunnel flow configuration can be varied

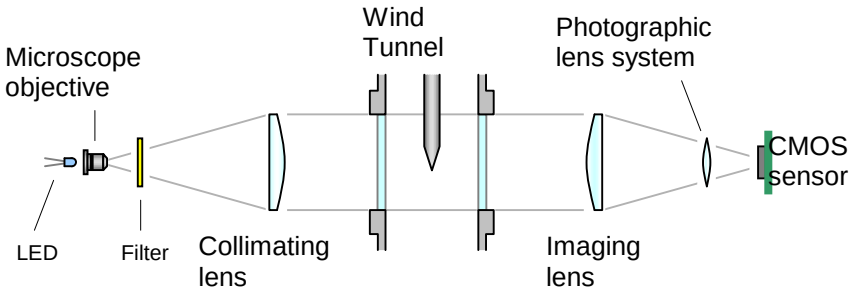


**Figure 2: Focused shadowgraphy system**

allowing testing of high-speed shock tracking. In the results shown here, the total pressure for the jet flow was varied generating a jet flow at Mach number varying between approximately $M_j$ = 0.9 (1.7 bar) and $M_j$ = 1.5 (3.7 bar).

The tunnel parameters for the results presented are as follows:

| | |
|---|---|
| Mach number | 2.06 |
| Total pressure | 105.5 kPa |
| Static pressure | 11.2 kPa |
| Total temperature | 311 K |

## FLOW VISUALIZATION

The focused shadowgraphy set-up used in the experiments described here is shown in Figure 2. It essentially consists of a light source, a microscope objective to expand the light beam, a second lens to produce a collimated beam going through the field of interest (e.g. wind tunnel test section) and a similar lens to collect the light directing it into a photographic lens system that is coupled to a CMOS detector. The use of a telescopic lens arrangement on the imaging side allows the focusing plane of the shadowgraphy system to be moved through the depth of the test volume by changing the position of the photographic lens and camera. Thus a sharp image of any object in the viewing area can be obtained. By adjusting the focus of the lens, the sharpness of the shocks as seen by the camera can be easily adjusted; by slightly defocusing, features can be made to show up more clearly.

The projection and imaging optics are mounted on a compact and portable optical breadboard system which can be positioned easily as two separate units on either side of the test facility (here a wind tunnel). The two separate units can be moved away for tunnel maintenance, and easily put back in position, maintaining alignment. The whole arrangement measures 2438 mm (96”) from end to end and the collimated beam section is 133 mm (5¼”) in diameter (determined by the diameter of the tunnel windows, the collimating and imaging lenses have a diameter of approximately 135 mm).

The camera is mounted at 90 degrees such that the wind tunnel flow is seen to be along the horizontal axis of the resulting image, from left to right.

Rather than using a discharge light source, such as a mercury arc lamp, a white LED is utilized. Unlike discharge sources, the solid-state device provides a stable and repeatable intensity level, with no jittering in its exact light emitting location. LEDs also offer long-life performance (>100,000 hours) in a compact package and can be pulsed quickly – typical rise times being less than 100ns.

The selected LED comprised a blue-emitting chip covered in a yellow-emitting phosphorous layer (Brookstone, 2003). To obtain a more even light distribution a yellow filter was placed after the microscope objective in order to block the blue component of the light emitted by such LEDs.

## SHOCK TRACKING

Shadowgraphy is based on the fact that light beams that travel through a medium with a variation in refractive index, as in compressible flows around an object, will be deformed and refracted (Merzkirch, 1987), bending towards the region of higher refractive index. This bending results in light and dark areas on the recording plane. In shadowgraphy of shock waves in a supersonic flow, the shock waves show up as narrow bands consisting of a light and a dark area. When shock waves around an object are studied, imaging the center plane of the object in a focused shadowgraphy system allows determining the shock location as the outer edge of the dark area. This forms the basis of the high-speed shock-tracking algorithm that was developed for this study (Bryanston-Cross *et al.*, 2003).

In the high-speed shock-tracking mode, only the last 4 rows of any 1280x8 frame delivered by the camera are considered. Four rows typically represent less than 0.5 mm in real terms (for the 5¼” viewing windows), so that shock curvature can be neglected for the conditions studied here, allowing reducing noise effects through averaging. Consequently, the data from the rows may be

vertically integrated to give a noise-reduced one-dimensional array (strip). To furthermore eliminate effects of variations in intensity caused by uneven illumination and steady dirt on e.g. the windows of the wind tunnel, strip-data taken before flow is present is subtracted from strip data from the same location with flow (and thus shocks). While running the camera in high-speed mode, each frame delivered by the camera is processed to find the position of shocks (Bryanston-Cross *et al.*, 2003). The resulting position data was plotted on screen, saved to disk and outputted electronically using an 8-bit D/A converter connected to the PC parallel port.

## NUMERICAL SIMULATION

A simulation of the supersonic flow around the aspirated nozzle is conducted using the high

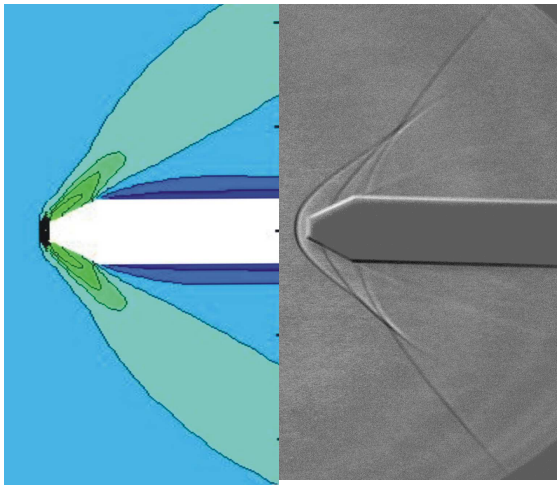

**Figure 3: Comparison: density plot of center-plane Navier-Stokes (left) vs. shadowgraphy (right). Still view, $M_t$=2 tunnel flow, no jet. 50 µs exposure**

accuracy NTS Navier-Stokes solver (see Shur et al., 2003), which is capable of solving flow conditions with a wide range of Mach numbers. Roe's (1981) flux difference splitting method is used. The solution is marched forward in time using a 2nd order implicit backwards differentiation.

The simulation is performed on a specially formed grid of approximately 400,000 nodes to take into account the cone shaped nozzle. The grid consists of two blocks: an inner and an outer block. The inner block's radial extent is in the region of 0.0001 – 0.005 m. The purpose of this block is to avoid a singularity at the axis. The simulation is run in unsteady mode needing around 10 sub-iterations per time step. Real time-step ($t$) is related to a non-dimensional time-step $t^*$ (where $t^* = t' v_0 / l_0$, where $v_0$ and $l_0$ represent the velocity and length scales respectively). Using a non-dime3nsional time-step of $t^*$ = 0.5 is found to be successful. All simulations are run in parallel OpenMP mode.

In the present study, free jet nozzle flows are not explicitly solved, but are treated by prescribing a suitable velocity profile as an inlet boundary condition. A power law velocity profile is specified at the jet outlet, the Mach number of the jet flow and the tunnel flow can each be at a maximum of 2.0. A sinusoidal disturbance is artificially added to the assumed mean velocity profile at the nozzle exit and normalized by the centerline inlet velocity. Near to the jet region a fine grid is used so as to resolve detailed flow structures. The results are circumferentially averaged.

## RESULTS

Figure 3 shows a comparison of the numerical and shadowgraphy results (still view) for the steady windtunnel flow around the nozzle (no jet flow). Note that the numerical result shows the density field in the center plane, whereas the shadowgraph is the result of light bending integrated over the full width of the flow field. Although due to this the shocks cannot be directly seen, the expansion wave at the junction of the cone with the main body can be identified. Furthermore, the bend in the bow shock seen in the shadowgraph is reproduced in the density field obtained numerically.

A comparison of results obtained for the tunnel flow combined with a steady jet flow is shown in Figure 4. Again, good correspondence is found between shape and position of both the bow shock

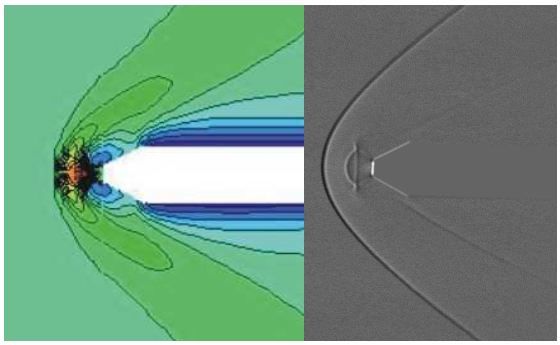

**Figure 4: Comparison: density plot NS (left, $M_t$=2, $M_j$=2) vs. shadowgraph $M_t$=2.06, $M_j$=1.5, still mode**

and the expansion wave. Also, the numerical result gives an indication for the causes for the particular shock-structure found between the bow-shock and the nozzle-exit. Behind the bow-shock a strong compression takes place, resulting in a small high-density region between the jet and the bow shock, apparently bordered by a high-density gradient.

Figure 5 shows a typical result obtained in the spatial-temporal mode for tunnel flow combined with a modulated jet flow. As can be seen, the result is a 'wobbly' image. This gives a misleading impression of irregularly shaped shock-waves, as

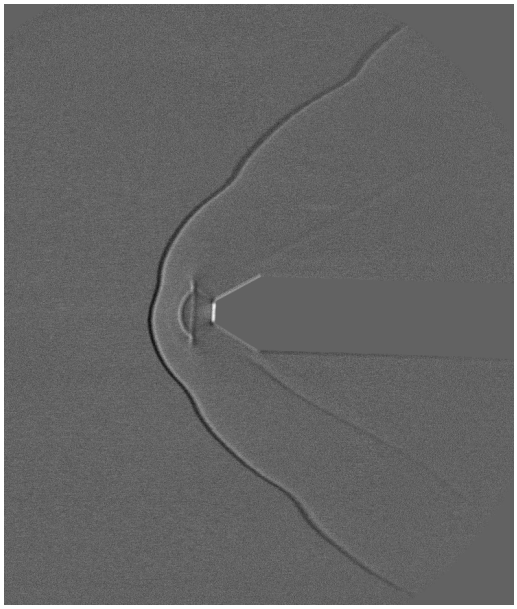

**Figure 5: Shadowgraphy result obtained in spatio-temporal mode. $M_t$=2.06, $M_j$~0.9-1.5, f~80 Hz**

the instantaneous still views of the same flow conditions show images similar to that in Figure 4, i.e. the shocks remain straight. Although the images obtained in this mode are thus not straightforward to interpret, the images also contain useful information that is not present in those obtained in the more conventional still-mode. Because the images contain both spatial as well as temporal information from Figure 5 it can be concluded that due to the jet-modulation, the bow-shock is moved to and from the jet nozzle. In Figure 5 about 6-7 oscillations are seen in the bow-shock; at a framing rate of 12 fps this would correspond to a frequency of [(1/12)/6.5]-1, i.e. ~78Hz. Note that the modulation frequency could only be set indirectly, and the resulting frequency could not be determined accurately from the valve motor. From the shock tracking experiments it was found that the set frequency was typically about 5% higher than the frequency determined from the tracking measurements. Thus, the number of oscillations in the image gives a reasonable estimate of the oscillation period in the flow based on the framing rate.

Apart from frequency information, also spatial information is obtained in this mode. From Figure 5 it can be seen that the bow-shocks are affected the strongest by the jet modulation, as shown by the clear periodicity. The effect also shows up in the shock closest to the bow-shock as well as in the ones originating close to the cone-cylinder transition. The diverging shocks going from the nozzle exit and the vertical shock at their endpoints (Mach-disk) do not show signs of unsteadiness.

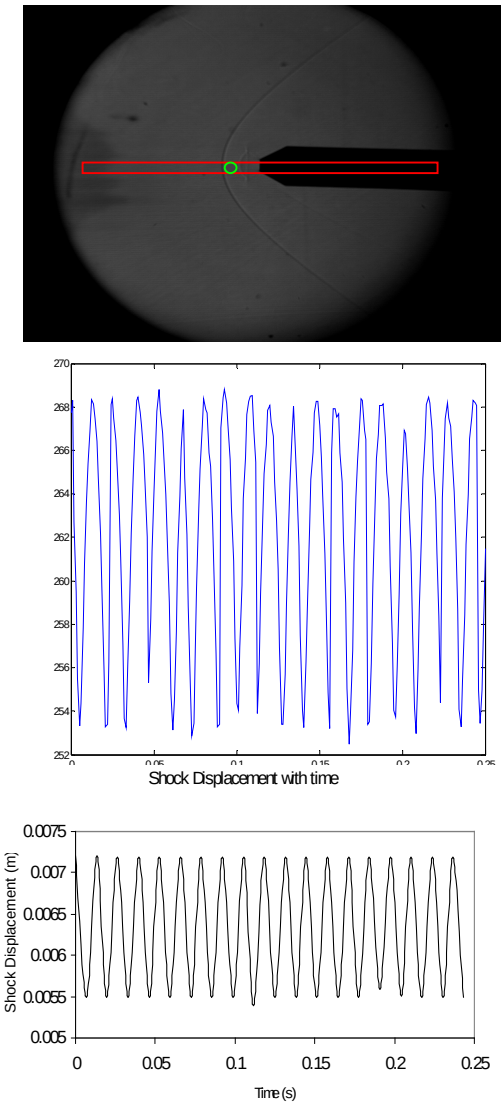


**Figure 6: Shock-tracking: shockposition vs. time for ~80 Hz oscillation. Top: shock position, middle: shadowgraph tracking, bootom: numerical result.**

Shock-tracking results for the modulation at 80 Hz nominally are shown in Figure 6, showing an actual shock modulation frequency of 76 Hz. The numerical result at this oscillation frequency indicates an amplitude of shock movement of approximately 1.7 mm, which corresponds very well with the tracking result of 16 pixels corresponding to ~2 mm.

## CONCLUSIONS AND DISCUSSION

The use of a low-cost CMOS sensor to achieve both full field-of-view mega-pixel flow visualizations as well as high-speed shock position tracking has been demonstrated in a low-cost digital focused shadowgraphy system tested on unsteady supersonic flow fields. The system uses

three recent advances in technology: a robust, low-cost ultra-bright white light LED as a light source; a CMOS camera for digital recording, allowing direct control over the size of the captured image, making it possible to trade size of image for image frame-rate; and fire-wire communications technology to transmit the images directly to a computer, which can then be used as input for a shock control system.

The light source can be modulated at high speed to give microsecond flashes, which allows freeze-frame imaging of unsteady events at a constant illumination level. The use of a CMOS camera enables data to be recorded in three basic modes of operation: a still full field-of-view freeze-frame mode, a windowed tracking mode and a continuous full field-of-view mode. This latter mode is based on the fundamental mode of operation of CMOS cameras and allows a new type of visualization to be obtained: spatial-temporal streak imaging. Although the images obtained in this mode are by no means trivial to interpret, they do help in the immediate identification of regions of instability.

Expanding the system with a second identical camera looking at the same flow region using a beam-splitter allows high-speed simultaneous tracking of features at different locations in the flow. Thus, e.g. the local angle of shock waves can be determined and monitored for changes.

As the CMOS camera uses FireWire connection, image processing can be performed immediately in the host computer. Thus, the system presented here can track the position of a flow feature at a rate of 980 Hz (determined by camera frame rate). This position information can be sent directly to a flow control-system, with a delay <100ms, allowing immediate feedback as input for a flow adjustment and controlling device, e.g. for controlling shock position in a supersonic inlet.

The constructed system is low cost (£1000 pounds for camera plus light-source) and can be generalized and miniaturized in several ways. Thus, it has the potential to be used e.g. for making an intra-passage transonic rotor shock measurement to provide active control within the gas turbine engine itself.

The results obtained with the shadowgraphy visualization and tracking system are confirmed and clarified by the numerical results. Good correspondence is found for shock positions, angle and oscillation.

## ACKNOWLEDGMENTS

The Warwick OEL team wishes to acknowledge Prof. A. Epstein for inviting them to participate in the research program at MIT. Part of this work was supported through a European Community Individual Marie Curie Fellowship 'An Intelligent Optical Diagnostic for Combustion' Contract no. HPMF-CT-2000-00997, by the UK Engineering & Physical Sciences Research Council (EPSRC), and by the US Defense Advanced Research Project Agency (DARPA). Furthermore, the authors acknowledge the advice of Prof Carpenter of Warwick University on flow conditions and the invaluable assistance of J. Letendre, J. Costa, V. Dubrowski, J. Head and D. Allaire of the Gas Turbine Laboratory of MIT in performing the experiments described in this paper.

## REFERENCES

Ben-Yakar, A., and Hanson, R.K., "Ultra-fast-framing schlieren system for studies of the time evolution of jets in supersonic crossflows," Experiments in Fluids 32, 652-666 (2002)

Brookstone Company Inc., Mexico MO, USA (purchased 2003)

Bryanston-Cross, P.J., Skeen, A.J., Timmerman, B.H., Dunkley, P., Paduano, J., Guenette, G.R., 'Low-cost digital visualization and high-speed tracking of supersonic shockwaves', Proc. SPIE Vol. 5191, Optical Diagnostics for Fluids, Solids, and Combustion II; Patrick V. Farrell, Fu-Pen Chiang, Carolyn R. Mercer, Gongxin Shen; Eds., Nov 2003, p. 156-165

DARPA, "Quiet Supersonic Platform (QSP)" (2003),http://www.darpa.mil/tto/programs/qsp.html

Donohoe, S.R. and Bannink, W.J., "Surface Reflective Visualizations of Shock-Wave/Vortex Interactions Above a Delta Wing," AIAA Journal 35(10), 1568-1573 (1997).

J. R. Gord, C. Tyler, K. D. Grinstead, G. J. Fiechtner, M. J. Cochran, and J. R. Frus, Imaging strategies for the study of gas turbine spark ignition, Optical Diagnostics for Fluids/Heat/Combustion and Photomechanics for Solids (SPIE, Denver, Co, USA, 1998), Vol. 3783, pp. 352-361.

Merzkirch, W., Flow Visualization, 2nd ed. (Academic Press, 1987).

Roe, P. L., 1981. Approximate Rieman solvers, parameter vectors and difference schemes. J. Comput. Phys. 46, 357-378.

Shur, M. L., Spalart, P. R., Strelets, M.Kh., Travin, A. K., 2003. Towards the prediction of noise from jet engines. Int. J. Heat Fluid Flow 24 (2003) 551-561

Timmerman, B.H., Holographic Interferometric Tomography for Unsteady Compressible Flows, PhD Thesis Delft University of Technology (Eburon P&L, Delft, the Netherlands, 1997).

Tucker P. G. 2004. Novel MILES computations for jet flows and noise, International Journal of Heat and Fluid Flow, In Press.